Printable Liquid-Metal@PDMS Stretchable Heater with High Stretchability and Dynamic Stability for Wearable Thermotherapy

Yuxin Wang, Zhe Yu, Guoyong Mao, Yiwei Liu, Gang Liu, Jie Shang, Shaoxing Qu, Qingming Chen,* and Run-Wei Li**

As a type of flexible electronics, wearable heaters have attracted broad attention because of their giant potential market value, such as for use in wearable thermotherapy. Wearable heaters are required to simultaneously possess high stretchability and dynamic stability, in order to realize joints or muscles thermotherapy during exercising. Here, a high-performance electrically driven heater using the conductive composite of liquid-metal (LM) and polydimethylsiloxane (PDMS) is reported, which is patterned as sinusoidal structure by the printing technology of direct ink writing. Because high conductive LM is chosen as the active material, the LM@PDMS stretchable heater possesses high stretchability (>100% strain) and good conductivity (1.81 × 10^3 S cm^{-1}). It also exhibits superb dynamic stability, due to the 3D conductive network of LM in matrix and the sinusoidal structure of the composite. While being stretched to the strain level of 100%, the heating temperature variation of LM@PDMS stretchable heater is less than 8%. This relatively low temperature variation is several times smaller than that of existing heaters at the same large strain levels. It is demonstrated that the LM@PDMS stretchable heater worn on the knee joint works well during strenuous exercise, thus proving great potential in wearable thermotherapy.

1. Introduction

In recent years, the wearable electrically driven heaters (WEDHs) based on Joule heating as a kind of flexible electronics have attracted broad attention due to their broad application, such as personal thermal management and wearable health-care devices.[1–5] Particularly, it has a giant potential market value using WEDHs for wearable thermotherapy.[6–9] It is a helpful physiotherapy for injured joints, muscles, and skins to relieve pain and recover their dynamism though continuous low-level heating, and is widely applicable to elder people, sedentary office workers, surgery patients, etc.[6,10–15] Because it will produce a large stretching strain (>50%) at joints and muscles when exercising,[12,16,17] the WEDH is required to possess high stretchability and stable dynamic heating property for thermotherapy application.

Y. X. Wang, Prof. Q. M. Chen
Faculty of Materials Science and Engineering
Kunming University of Science and Technology
Kunming 650093, P. R. China
E-mail: chenqm@kmust.edu.cn, chqm99@yahoo.com

Y. X. Wang, Z. Yu, Dr. Y. W. Liu, Prof. G. Liu, Prof. J. Shang, Prof. R.-W. Li
CAS Key Laboratory of Magnetic Materials and Devices
Ningbo Institute of Materials Technology and Engineering
Chinese Academy of Sciences
Ningbo 315201, P. R. China
E-mail: shangjie@nimte.ac.cn; runweili@nimte.ac.cn

Y. X. Wang, Z. Yu, Dr. Y. W. Liu, Prof. G. Liu, Prof. J. Shang, Prof. R.-W. Li
Zhejiang Province Key Laboratory of Magnetic Materials and Application Technology
Ningbo Institute of Materials Technology and Engineering
Chinese Academy of Sciences
Ningbo 315201, P. R. China

Z. Yu
College of Materials Science and Opto-Electronic Technology
University of Chinese Academy of Sciences
Beijing 100049, P. R. China

Dr. G. Mao, Prof. S. Qu
State Key Laboratory of Fluid Power and Mechatronic System
Key Laboratory of Soft Machines and Smart Devices of Zhejiang Province
Department of Engineering Mechanics
Zhejiang University
Hangzhou 310027, China

The ORCID identification number(s) for the author(s) of this article can be found under https://doi.org/10.1002/admt.201800435.

DOI: 10.1002/admt.201800435

To meet these requirements, a series of stretchable WEDHs with unique stretchable structure have been reported,[3,5,6,10–12,18] including the wrinkled,[3] knitted,[12] fractal,[6] and similar patterns. The stretchability of them is usually between 30% and 100% strain, while the heating temperature changes significantly during stretching.[2,6,8,10–12,19–21] For instances, Hong et al. prepared a stretchable heater based on percolation network of silver nanowire, wherein the heating temperature changes from 80 to 50 °C while being stretched to the strain level of 30% strain[2]; Lee et al. prepared a stretchable heater based on surface wrinkle of carbon nanotube sheet, thereof the heating temperature changes from 200 to 150 °C while stretching to 100% strain.[3] Due to the fact that the active materials of existing stretchable WEDH are solid fillers, e.g., metal nanowire,[2,6,10–23] carbon nanomaterial,[3,12,19,24–27] and intrinsically conductive polymer,[11,28] embedded in elastic matrix, their electrical resistances are sensitive to the stretching strain and lead to a large variation of electronic performance during stretching.[29] Therefore, it is the key of stretchable WEDH for wearable thermotherapy to obtain a conductor that simultaneously possesses high stretchability and high dynamic stability, i.e., the electrical and heating properties are stable during stretching.

In this paper, we report a high-performance stretchable WEDH made of a conductive composite of liquid-metal (LM) and polydimethylsiloxane (PDMS). The LM@PDMS composite is patterned as sinusoid of serpentine structure by the printing technology of direct ink writing (DIW). Because LM is a mobile liquid conductor at room temperature (RT), filling LM in elastic matrix has less impact on the mechanical property of matrix. The as-prepared LM@PDMS stretchable WEDH exhibits high stretchability (>100%) and good conductivity (1.81×10^3 S cm^{-1}). Importantly, LM@PDMS stretchable WEDH has superb dynamic stability of electrical and heating properties. For example, when being stretched to the strain level of 100%, the variations of its electrical resistance and heating temperature are lower than 5% and 8%, respectively. Its temperature variation is several times smaller than that of the reported stretchable heater at the same working voltage and large stretching strain. There are two reasons for the superb dynamic stability: LM forms a micro-3D conductive network in PDMS matrix and the pattern of LM@PDMS composite is designed as a suitable sinusoidal structure. Furthermore, it is demonstrated that prepared LM@PDMS stretchable WEDH worn at knee joint works well for thermotherapy, even if doing strenuous exercise.

2. Results and Discussion

LMs based on gallium, such as eutectic gallium indium (EGaIn) and gallium-indium-tin ("galinstan," GaInSn) alloys, have emerged recently as important conductive candidates for flexible and stretchable electronics.[29–32] It has been demonstrated that the conductive composite filled with LM exhibits high conductivity and dynamic electrical stability by designing 3D conductive network of LM in elastic matrix.[29,33,34] To this conductive composite filled with LM reaching a percolation threshold, it could be separated into two phases: a rich region of elastic matrix embedding LM and a continues rich region of LM (conductive network).[29,35–37] While stretching, the rich region of elastic matrix forms an elastic microstructured strut, and the rich region of LM maintains stable electrical conduction.[29–31,36,37] Therefore, it could show high performances to as a perfect material for stretchable WEDH. But the raw materials of composite are all liquid before thermal curing, which leads to difficulty in patterning complex structure.[29,32] In the patterning technology, printing is a useful method with low cost and high efficiency,[38–41] such as DIW.[42–44] The LM@PDMS stretchable WEDH is prepared by DIW, as shown in **Figure 1**a. First, the mushy LM@PDMS is patterned on a PDMS film using air injection, and mushy LM@PDMS is the mixture of LM and uncured PDMS. Next, the patterned mixture is cured at 60 °C to obtain LM@PDMS composite after standing for 30 min. Then, the LM@PDMS composite is encapsulated by PDMS. Finally, LM@PDMS stretchable WEDH with designed pattern is obtained by peeling off from mold. The important preparation parameters and detailed preparation craft can be found in the Experimental Section. Importantly, the LM filling volume fraction of LM@PDMS composite is at high level (70 vol%). At the low-level filling fraction, the patterned composite will flow like water leading to widen the width of printed line and destroy the original pattern. When the filling fraction of LM reaches a high level of 70 vol%, the widening of line width can be ignored (Figure S1, Supporting Information). The reason is that the internal friction between these two liquid phases increases to oppose the flow of LM@PDMS composite as there is increase in LM filling fraction. Furthermore, the rheological properties of the printing inks at different LM filling ratios were tested by a rotational rheometer. The results are shown in Figure S2 of the Supporting Information. It was tested by rotational rheometer. From Figure S2a (Supporting Information), it can be found that the shear modulus, including storage modulus (G') and loss modulus (G''), increases with the increase of LM filling ratios. At the low-level filling fraction (<40 Vol%), the G' is lower than G'' during testing shear stress, which means the inks are the liquid state. At the high-level filling fraction (>60 Vol%), the G' is higher than G'' during low testing shear stress. But during large testing shear stress, its G' is lower than G'', which is caused by yield phenomena. It means the static inks with high filling fraction are the solid state, and they are the liquid state under large shear stress. Therefore, the inks with high filling fraction can flow readily through fine nozzles and keep the line shape after injecting. This result is similar to Figure S1 (Supporting Information). According to Figure S2a,b (Supporting Information), we think the rheological property of ink at 70 Vol% is best suited for printing.

The photo of sample with a complex fractal pattern is shown in Figure 1b, and the width and height of printed line are about 400 and 230 µm, respectively (Figure 1c). From the inset of Figure 1c and Figure S3a of the Supporting Information, it can be found that the LM has formed a continuous 3D conductive network microstructure in the PDMS matrix. This network structure is similar to 3D calabash bunch previously reported, which improves the dynamic stability of LM@PDMS composite.[29] According to electrical test results of printed LM@PDMS composite (a straight line), its conductivity is as high as 1.81×10^3 S cm^{-1}, but its resistance variation is not as small as expected during stretching ($\Delta R/R_0$ = 18.29% @ 100%

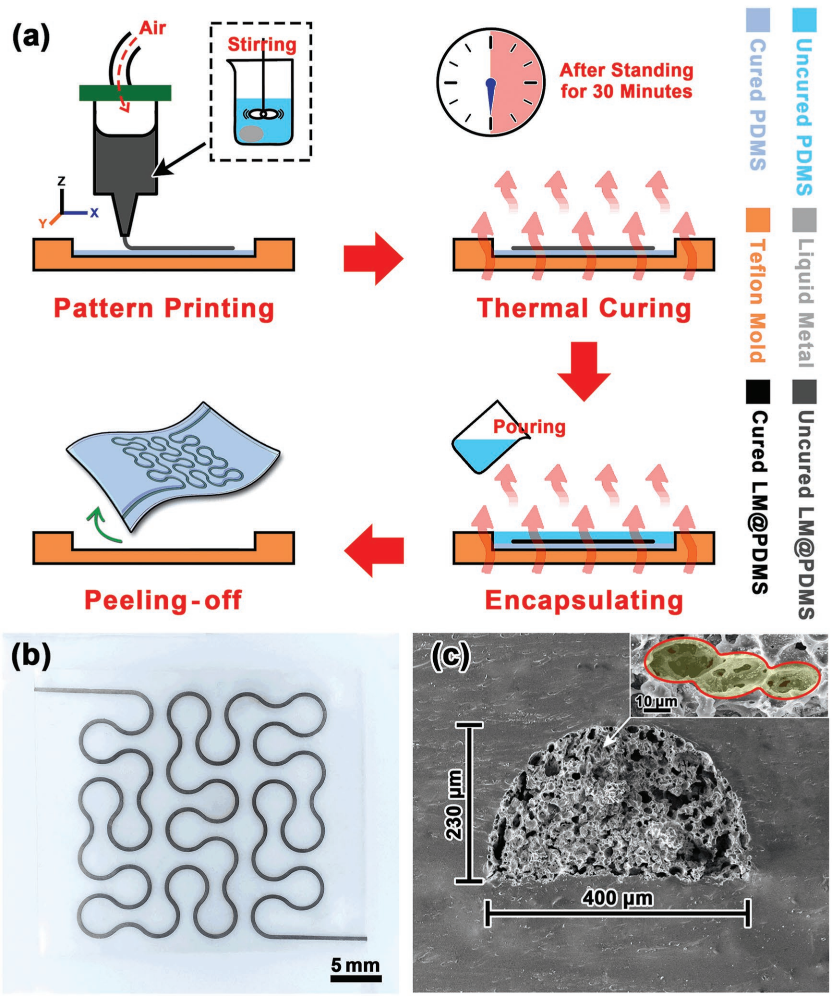

Figure 1. a) Schematic illustration of the fabrication procedure for preparing LM@PDMS stretchable WEDH. b) Optical photo of prepared sample with complex fractal structure. c) Cross-sectional view SEM image of the line of LM@PDMS stretchable WEDH. The inset shows its internal microstructure of 3D calabash bunch network.

strain; Figure S4 of the Supporting Information). It seems that these calabash bunches of initial state have undergone minor deformation, which is caused by the resistance force from the injection head of syringe barrel (Figure S3b, Supporting Information).

To improve dynamic electrical stability of printed LM@PDMS composite, its structure is designed as a sinusoid of serpentine structure, as shown in **Figure 2**a. As we know, with increasing amplitude height and decreasing period length, the dynamic stability of composite with sinusoidal structure improves, but its initial resistance also increases, which is disadvantageous for WEDH working under low voltage. The ratio of amplitude height to period length (A/P) is considered as an important parameter to explore the most suitable sinusoidal structure. The initial resistances of printed composite and its resistance variations at 100% stretching strain were tested at different A/P. In this part, the distance between A and B points in Figure 2a, i.e., the linear distance of sinusoid, is constant, and related electrical experiments were tested on the two points. It can be found that the optimal A/P of sinusoidal structure is about 0.6 from the results (Figure 2b). At this A/P, the printed LM@PDMS composite with sinusoidal structure exhibits low initial resistance (R_0 = 8.70 Ω) and small resistance variation during stretching ($\Delta R/R_0$ = 4.23% @ 100% strain). Compared with pure PDMS embedding LM wire with serpentine structure ($\Delta R/R_0$ = 30%–45% @ 100% strain),[45] printed LM@PDMS composite with optimal sinusoidal structure still exhibits a superb dynamic stability, because of the 3D conductive network microstructure of LM in PDMS. This can be seen visually from Figure S5 of the Supporting Information. When sinusoidal composite with A/P of 0.6 is stretched to 50% strain, the light intensity of LED connecting with it does not change significantly. In addition, finite element analysis (FEA) is performed to simply simulate the stretching process of sinusoidal structure samples with different A/P. As shown in Figure S6a of the Supporting Information, the Young's modulus of pure LM@PDMS film is about tenfold lower than that of pure PDMS film, which means the deformability of LM@PDMS composite is better than that of pure PDMS matrix. From the results of the simulation, it can be observed that the stretching strain will induce the increase of the width of the LM@PDMS with sinusoidal structure (Figure S6b, Supporting Information), which enhances the final conductivity compared to that with straight structure. A similar situation can be found in the optical photos of sample before and after stretching (Figure S6b, Supporting Information). In the inset of Figure S6c, we plotted the relative resistances of LM@PDMS with different A/P sinusoidal structure at 0% stretching strain and 100% stretching strain. With increasing of A/P, the relative resistances of the stretched LM@PDMS (100% strain) decrease with the increase of A/P, but their initial relative resistances (0% strain) increase. We calculated the average relative resistances of the initial and the stretched LM@PDMS, shown in Figure S6c (Supporting Information). It is found that the average resistances will decrease first and then increase as there is increase in the A/P. The minimal resistance occurs when A/P is between 0.4 and 0.6, which is the same as the observation in experiments. In this simulation, the thickness variation is neglected. Taken together, it is sure that sinusoidal structure with the A/P of 0.6 is really optimal sinusoidal structure in our existing understanding.

Furthermore, the dynamic electrical property of LM@PDMS composite with optimal sinusoidal structure is further evaluated under different stretching conditions, including load–unload operation, stretching velocity, and stretching cycle. At various load–unload operations, the resistance variation of sample is stable and the electrical hysteresis coefficients are all lower than 0.083, as shown in Figure 2c. When sample is

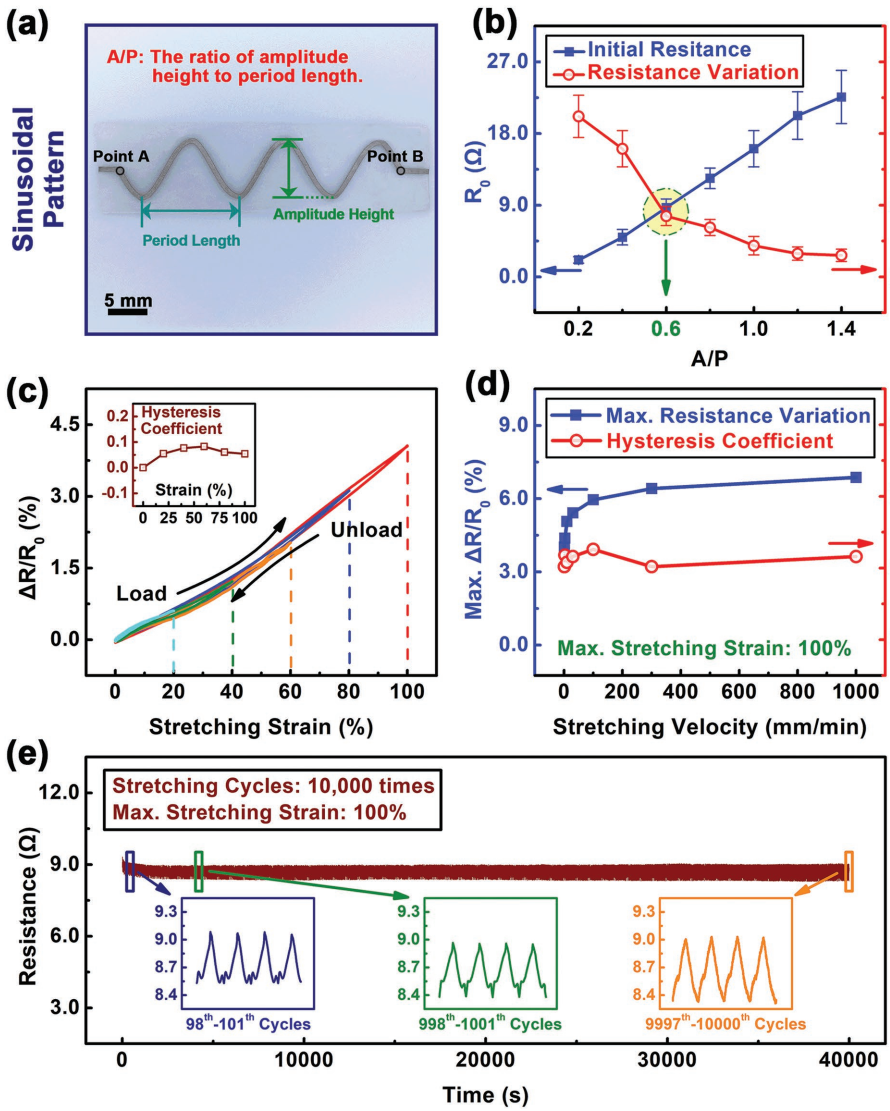

Figure 2. a) Optical photo of printed LM@PDMS sample with sinusoidal structure. b) Initial electrical resistance of sample with sinusoidal structure and its resistance variation at 100% strain as a function of the A/P. The A/P is the ratio of amplitude height to period length in sinusoidal structure. c) Relative resistance variation as a function of stretching strain during various load–unload operations. The inset shows the electrical hysteresis coefficient of the load–unload curves. The A/P of testing sample's sinusoidal structure is 0.6. d) Maximum relative resistance variation and electrical hysteresis coefficient as a function of stretching velocity. The A/P of testing sample's sinusoidal structure is 0.6. e) Resistance evolution of LM@PDMS with optimal sinusoid structure under repeated stretching cycle operations (10 000 times). The insets are several representative stretching cycles.

stretched to 100% strain by different stretching velocities, its resistance variation increases with increasing stretching velocity, but it begins to be stabilize at high stretching velocity ($\Delta R/R_0$ = 6.87% @ 1000 mm min^{-1}; Figure 2d). In Figure 2d, it can also be found that the electrical hysteresis coefficient of sample is influenced less by the stretching velocity, which fluctuates between 0.051 and 0.063. Finally, the resistance evolution of sample was recorded during repeat stretching cycles for 10 000 times, when the maximum stretching strain is 100%. As shown in Figure 2e, the resistance of sample decreases slightly from 8.88 to 8.30 Ω under unstrained state. As there is increase in stretching cycles, the curve of electrical resistance-stretching strain tends to be smooth, which may be due to the fact that the internal structure of LM@PDMS composite appears a preferred orientation along the stretching direction. Taken together, the printed LM@PDMS composite with optimal sinusoidal structure (A/P = 0.6) exhibits a high conductivity and a superb dynamic electrical stability, so it can be thought that such an LM@PDMS composite is very suitable as a stretchable WEDH for wearable thermotherapy.

The Joule heating property of LM@PDMS stretchable WEDH with optimal sinusoidal structure was investigated. The test results under unstrained state are displayed in **Figure 3**. In Figure 3a, stepwise voltage from 0.5 to 3.5 V is applied to the sample, and the temperature of sample rises up with increasing applied voltage. Figure 3b shows the various infrared (IR) thermal images for different applied voltages, wherein the heating temperatures are recorded by an IR camera. It can be

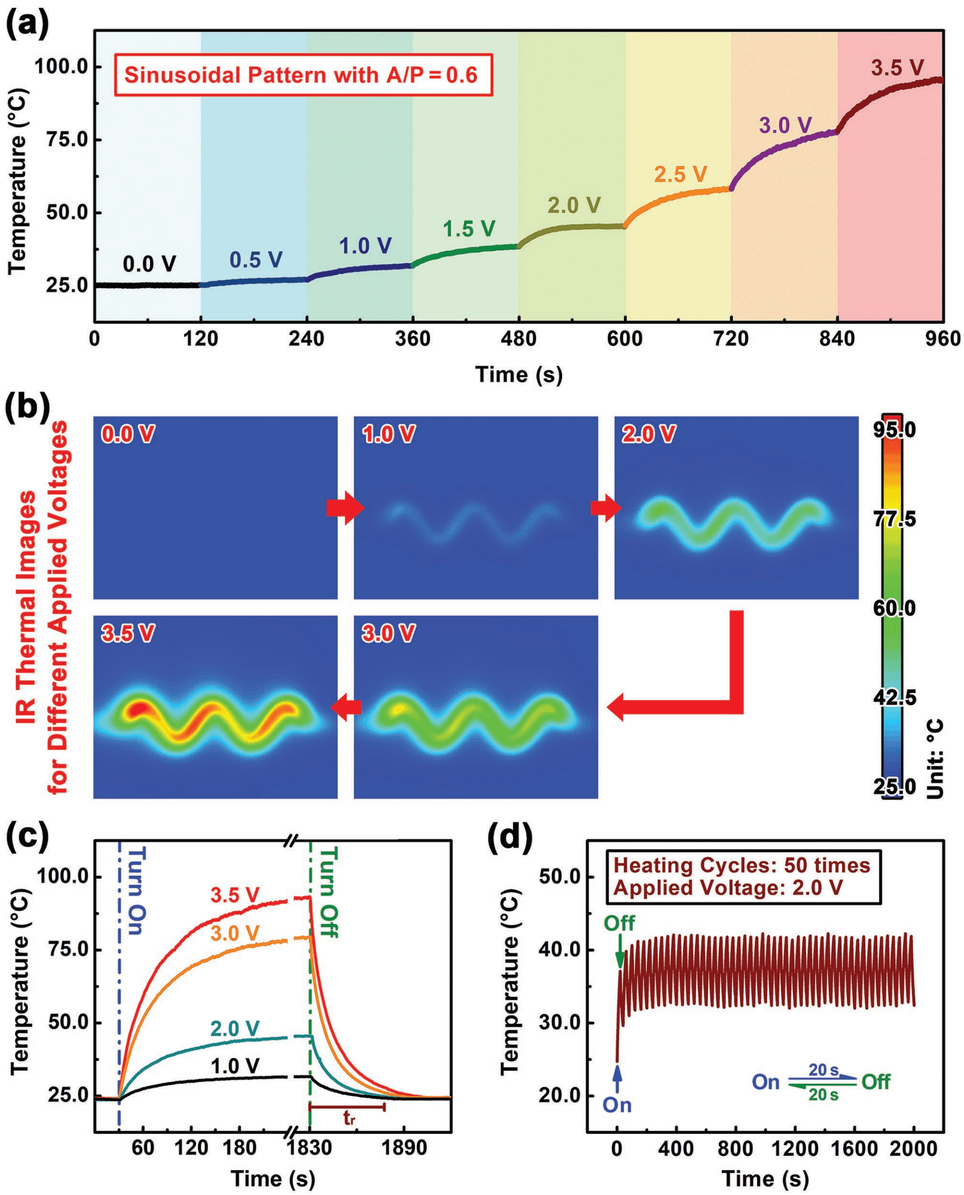

Figure 3. a) Temperature evolution of LM@PDMS stretchable heater with optimal sinusoidal structure under stepwise voltage from 0.5 to 3.5 V. b) IR thermal images of sample with optimal sinusoidal structure for different applied voltages. c) Temperature evolution of sample with optimal sinusoidal structure applied different voltages for long time. d) Temperature evolution of sample with optimal sinusoidal structure under repeated heating cycle operations (50 times).

found that the saturated temperature (T_s) can be easily driven up to 45.26 and 95.9 °C, when applied voltages of 2.0 and 3.5 V, respectively. For practical applications, heating stability and reliability of a heater are also important, while applying a voltage on it for a long time. The sample is applied various voltages for 30 min, and then the voltage is turned off. The temperature evolutions in this process are shown in Figure 3c. It can be found that when sample has been applied various voltages, its heating temperature only increases 1.45%–3.64% relative to that at an applied time of 3 min (Figure 3c). After turning off input voltages, the sample is cooled to RT (25 °C), and the recovery times (t_s) are between 20.44 and 56.20 s (Figure 3c) under various voltages. Meanwhile, heating cycle was conducted on sample for 50 times. At each time cycle, the sample was applied a voltage of 2 V for 20 s and then the input voltage was turned off to naturally cool for 20 s. Although there is a residual heat on the sample leading to a phenomenon that the cooling temperature of sample can return to the RT at short time, the lowest cooling temperature and highest heating temperature will be stable around at 32.5 and 41.7 °C, respectively, after several heating cycles (Figure 3d). According to the heating property of LM@PDMS stretchable WEDH under unstrained state, it basically meets the requirement of continuous low-level heating (40–77 °C)[11] for wearable thermotherapy.

Importantly, the results of its heating property are shown in **Figure 4**, when LM@PDMS stretchable WEDH with optimal

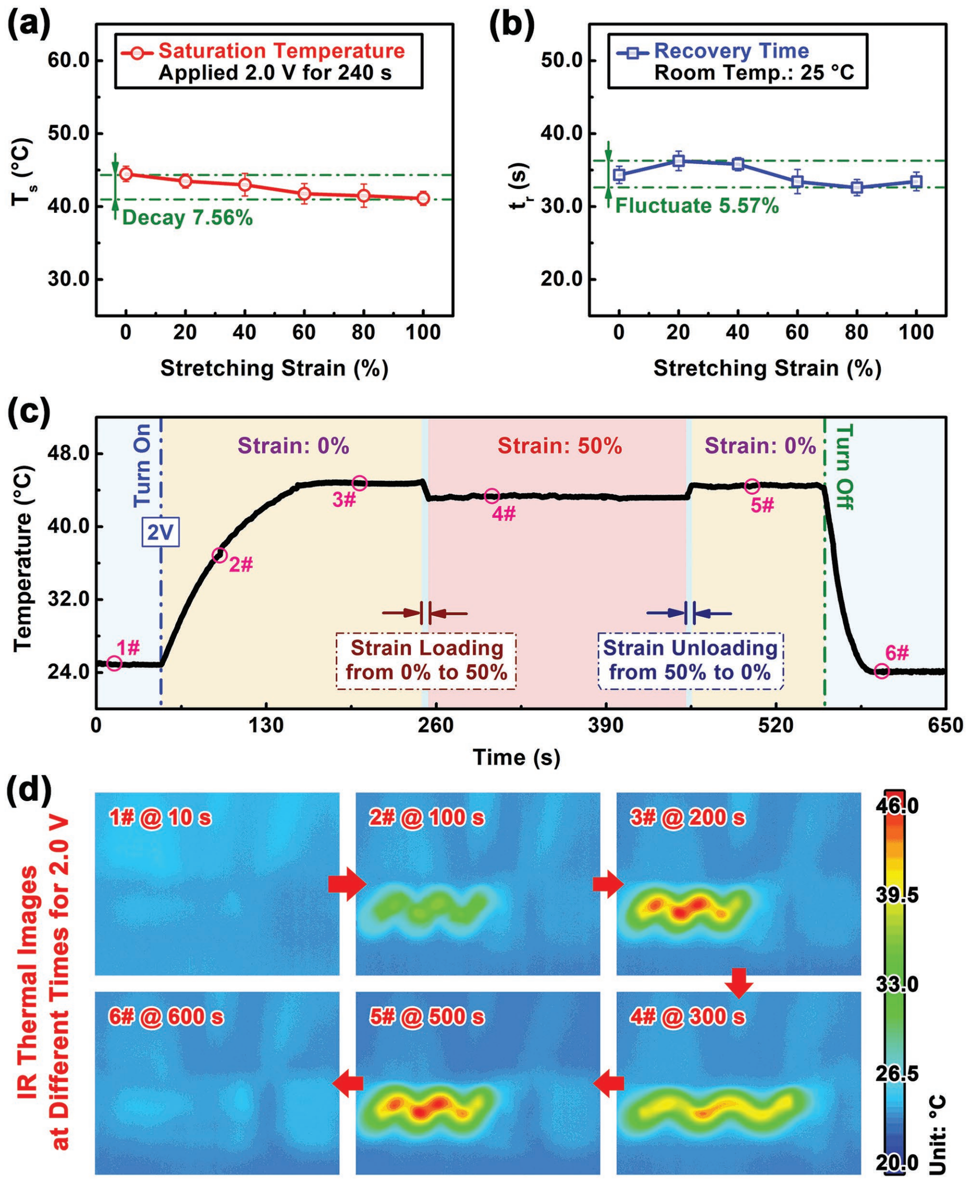

Figure 4. a) Saturation temperature of LM@PDMS stretchable heater with optimal sinusoidal structure as a function of stretching strain. b) Cooling recovery time of sample with optimal sinusoidal structure as a function of stretching strain. c) Temperature evolution of sample with optimal sinusoidal structure at the first of repeated dynamic hybrid cycle operations. Temperature evolutions at rest dynamic cycles are shown in Figure S7 of the Supporting Information. d) IR thermal images of sample with optimal sinusoidal structure at six representative moments of first cycle. Six moments are marked in (c).

sinusoidal structure is stretched to large strain. Owing to superb dynamic electrical stability of sample, the T_s of sample decreases slightly with increased stretching strain (Figure 4a). Even if the sample is stretched to 100% strain, the relative variation of T_s is only 7.56% for applying a voltage of 2 V. From Figure 4b, it can be seen that there is an unnoticeable effect of stretching strain on t_s of sample, which fluctuates within a narrow range of 5.57%. In order to better evaluate dynamic stability of heating property, the temperature evolutions of sample were recorded during dynamic hybrid cycles of 50 times. Each dynamic hybrid cycle is consisted of three stages: first applying 2 V voltage on sample to T_s, then loading and unloading strain on sample, and lastly turning off input voltage to cool sample for 100 s. Figure 4c shows the temperature evolution of sample in the first dynamic hybrid cycle, and Figure 4d shows the IR thermal images of sample at six representative moments (marked in Figure 4c) in the first cycle. It can be found that the T_s is still stable at a range of 43.15–44.93 °C during loading and unloading strain. As shown in Figure S7 of the Supporting Information, the temperature evolution of sample in the rest of dynamic hybrid cycles is similar to that in the first cycle. In short, prepared LM@PDMS stretchable WEDH also meets the dynamic stability requirement of wearable thermotherapy. It is important to ensure there is a fine thermotherapy effect in the process of exercising.

As shown in **Table 1**, compared with the typical recently reported stretchable WEDH, prepared LM@PDMS

Table 1. Comparison table of our LM@PDMS stretchable WEDH with the reported stretchable WEDH.

Active materials	Voltage for 50 °C	Stretchability	Relative temperature variation @ stretching strain	Ref.
Ag nanowire	2.8 V	60%	37.50% @ 30% strain	[2]
Ligand-exchanged Ag nanowire	0.75 V	100%	12.18% @ 50% strain	[6]
Cu nanowire fiber	2 V	100%	37.74% @ 80% strain	[10]
Metallic glasses CuZr	<3 V	≈70%	16.67% @ 70% strain	[8]
Carbon nanotube sheet	>10 V	>300%	33.33% @ 100% strain	[3]
Carbonized modal textile	1.5 V	70%	16.67% @ 70% strain	[12]
Graphene fiber	2.5 V	≈33%	85.90% @ 33% strain	[19]
PEDOT:PSS	<3 V	>30%	10% @ 30% strain	[11]
Liquid-metal galinstan	2.0 V	>100%	7.56% @ 100% strain	This work

stretchable WEDH shows preponderant performance in terms of high stretchability and super dynamic stability of heating property. Under the same stretching state, the heating temperature variation of our heater is several times smaller than that of reported stretchable heater.[2,3,6,8–12,15,19–21,24] In addition, our DIW preparation method is very suitable to rapidly obtain a specially designed stretchable heater for thermotherapy, which has a pattern compliant with the type of exercise at different human parts. To show the advantage of this prepared method, an LM@PDMS stretchable WEDH was prepared to do thermotherapy for knee joint, as shown in **Figure 5**a. Because there is a simple uniaxial stretching strain at knee, the pattern of heater is designed as a palisade shape with sinusoidal structure, and the heater is embedded in the kneepad. In the demonstration, a volunteer rode the exercise bicycle with this kneepad. In Figure 5b, it shows the four photos of actual motion and corresponding IR thermal images, when the knee moved to the top, front, bottom, and back of the whole exercise. From the IR thermal images, it can be seen that the heating temperature of this LM@PDMS stretchable WEDH is almost same during exercising. No matter how fast the volunteer rode, its dynamic heating property is also extremely stable (Video S1, Supporting Information).

3. Conclusion

In summary, we reported a stretchable wearable electrically driven heater using LM@PDMS conductive composite, which is patterned as a sinusoidal structure by the DIW. It is sure that the optimal sinusoidal structure is at the A/P of 0.6 according to the experimental tests and FEA. Because high conductive LM is chosen to replace traditional solid material as active material, LM@PDMS stretchable heater simultaneously possesses high stretchability (>100% strain) and good conductivity (1.81×10^3 S cm^{-1}). Importantly, owing to the 3D conductive network microstructure of LM in matrix and printed sinusoidal structure pattern of LM@PDMS composite, the heater exhibits superb dynamic stability of electrical and heating properties. Even if stretching to 100% strain, its electrical resistance and heating temperature only change 4.23%

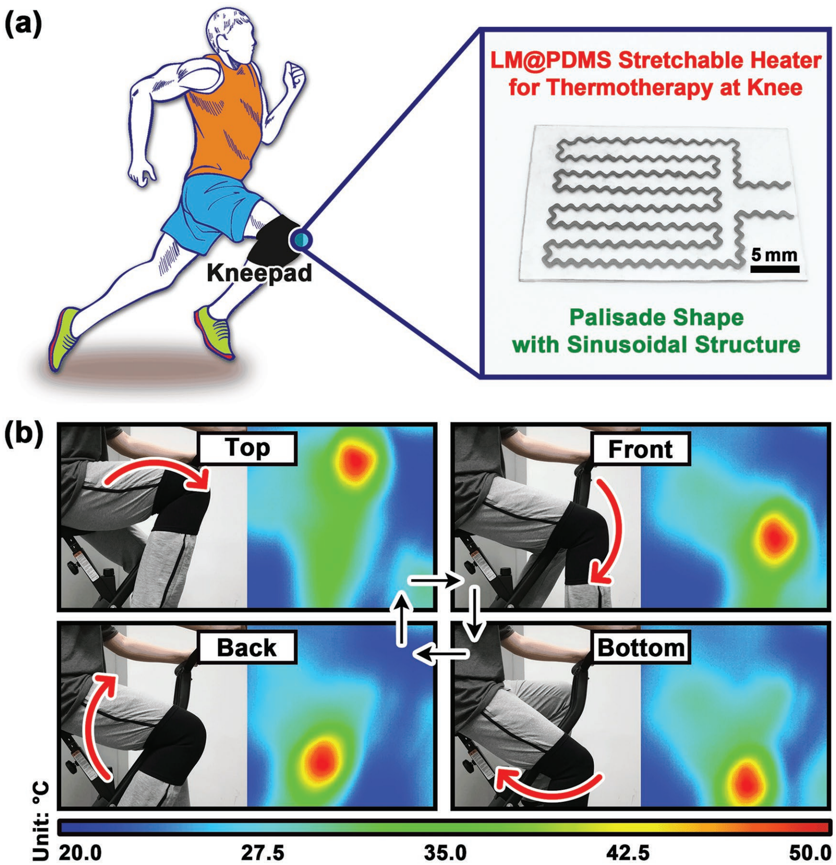

Figure 5. a) Optical photo of specially designed LM@PDMS stretchable WEDH and schematic illustration of its working condition. The pattern of this heater is palisade shape with sinusoidal structure in order to do thermotherapy on knee. b) Optical photos of exercise at different states and corresponding IR thermal images. Kneepad worn by volunteer is embedded with the LM@PDMS stretchable WEDH of (a).

ADVANCED MATERIALS TECHNOLOGIES
www.advmattechnol.de

and 7.56%, respectively, which is several times smaller than the reported stretchable heater. Its high stretchability, good conductivity, and superb dynamic stability promise its superior performance for wearable thermotherapy. It has been demonstrated well that the heating temperature is stable when a volunteer worn the kneepad embedding a prepared LM@PDMS stretchable heater to do exercise. In addition, it is noteworthy that our DIW preparation method is a low-cost and highly efficient way to obtain a special complex pattern. It means the LM@PDMS stretchable heater will be compliant with the deformation type of different parts of body by designing its pattern. We believe that this work will contribute to the development of stretchable heater for wearable thermotherapy.

4. Experimental Section

Preparation of Liquid-Metal Galinstan and Patterned LM@PDMS Stretchable Heater: The liquid-metal galinstan was synthesized from high purity metal gallium (99.99%; Beijing Founde Star Sci. & Technol. Co., Ltd), indium (99.995%; Beijing Founde Star Sci. & Technol. Co., Ltd), and tin (99.99%; Beijing Founde Star Sci. & Technol. Co., Ltd) by mixing and stirring under 60 °C. The mixing ratio of Ga, In, and Sn is 68.2:21.8:10 by mass. Then, the synthetic galinstan and PDMS (Sylgard 184, Dow Corning Corporation) were mixed in the volume ratio of 7:3 by using an electric mixer (WB3000-D, WIGGENS) at a speed of 100–200 rpm for 30 min. After mixing uniformly, the mushy LM@PDMS mixture was loaded into the syringe barrel of dispenser (Ultimus Precision Fluid Dispenser, EFD) with an injection head of 0.38 mm diameter. The dispenser with digital pneumatic regulator was connected with air bottle to extrude out the mixture, and the syringe barrel with tapered dispenser tip was connected with a three-axis motion numerical controlled platform (AMCNC-01, Armok Engraving Machines). Controlling the moving velocity of syringe barrel between 180 and 240 mm min^{-1} and the air pressure between 200 and 400 Pa, the mushy mixture was directly printed on the PDMS film in a teflon mold. Next, the patterned LM@PDMS composite stood for 30 min and then was cured at 80 °C for 2 h. Afterward, the liquid PDMS was poured in mold and cured quickly at temperature of 120 °C to encapsulate the patterned LM@PDMS composite. The purpose of encapsulating is to prevent the LM leaching out from the composite. Last, the LM@PDMS stretchable heater was obtained after peeling off from mold. In order to prevent the leaking of LM from electrical interface, the soft conductive composite based on PDMS filled with vertically aligned columns of Ag-coated Ni microparticles was used as the electrical via of our heater to connect with copper wires of external circuit. This material has been proved as a good electrical via for LM circuit.[46]

Characterization of the Microstructure: The cross-sectional microstructures of samples were characterized by the field-emission scanning electron microscopy (Sirion 200, FEI).

Rheology Measurements: The rheological properties of the printing inks at different LM filling ratios were characterized by a rotational rheometer (Physica MCR-301, Anton Paar) at RT. During testing, the storage modulus, loss modulus, and apparent viscosity were recorded simultaneously, while oscillatory measurements were carried out at a frequency of 1 Hz within the shear strain of 0.1%–100%.

Measurements of Electrical and Heating Properties: The resistance of LM@PDMS stretchable heater was measured by the four-wire method using the DC current source (6221, Keithley) and the nanovoltmeter (34420A, Agilent). The stretching strain was applied by a universal material testing machine (5943, Instron). The heating temperature variation of heater was tracked by an IR camera (T630sc, FLIR).

Finite Element Analysis: The deformation of the LM@PDMS with sinusoidal structure subject to stretching was simulated with the finite-element software ABAQUS. In the simulation, the PDMS and LM@PDMS are both considered as incompressible hyperelastic material (Neo-Hookean Material) and the PDMS is well bonded with the LM@PDMS. Then, the deformed LM@PDMS with sinusoidal structure was transferred to another finite-element software (COMSOL Multiphysics) to calculate the resistance by considering the LM@PDMS as a homogenous material with consistent resistivity.

Thermotherapy for Knee Joint: To understand the thermotherapy effect during exercise, the temperature changes from two healthy adult volunteers were characterized using an IR camera in real-time. The thermotherapy kneepad with prepared heater was worn on the knee joints of volunteers. All volunteers took a 10-min rest before the measurement, and the thermotherapy effect was measured after riding the exercise bicycle for 5 min. The two subjects (age: 25 ~ 30.5 years) were coauthors and all work involved informed consent from the subjects.

Supporting Information

Supporting Information is available from the Wiley Online Library or from the author.

Acknowledgements

Y.X.W. and Z.Y. contributed equally to this work. This research was partially supported by the National Natural Foundation of China (Grant Nos. 61774161, 61704177, 51525103, and 11474295), the China International Cooperation Project (Grant No. 2016YFE0126700), the National Key Technologies R&D Program of China (Grant No. 2016YFA0201102), the Public Welfare Technical Applied Research Project of Zhejiang Province (Grant No. 2017C31100), the Ningbo Science and Technology Innovation Team (Grant No. 2015B11001), the Natural Science Foundation of Ningbo (Grant Nos. 2017A610093 and 2017A610097), and Ningbo Major Science and Technology Projects (Grant No. 2017B10018).

Conflict of Interest

The authors declare no conflict of interest.

Keywords

direct ink writing, dynamic stability, liquid-metal, stretchable heater, wearable thermotherapy

Received: September 11, 2018
Revised: October 10, 2018
Published online:

[1] S. Yao, J. Cui, Z. Cui, Y. Zhu, *Nanoscale* **2017**, *9*, 3797.
[2] S. Hong, H. Lee, J. Lee, J. Kwon, S. Han, Y. D. Suh, H. Cho, J. Shin, J. Yeo, S. H. Ko, *Adv. Mater.* **2015**, *27*, 4744.
[3] Y. Lee, V. T. Le, J.-G. Kim, H. Kang, E. S. Kim, S.-E. Ahn, D. Suh, *Adv. Funct. Mater.* **2018**, *28*, 1706007.
[4] T. Q. Trung, N.-E. Lee, *J. Mater. Chem. C* **2017**, *5*, 2202.
[5] Q. Liu, J. Huang, J. Zhang, Y. Hong, Y. Wan, Q. Wang, M. Gong, Z. Wu, C. F. Guo, *ACS Appl. Mater. Interfaces* **2018**, *10*, 2026.
[6] S. Choi, J. Park, W. Hyun, J. Kim, J. Kim, Y. B. Lee, C. Song, H. J. Hwang, J. H. Kim, T. Hyeon, D.-H. Kim, *ACS Nano* **2015**, *9*, 6626.

[7] Y.-Q. Li, W.-B. Zhu, X.-G. Yu, P. Huang, S.-Y. Fu, N. Hu, K. Liao, *ACS Appl. Mater. Interfaces* **2016**, *8*, 33189.
[8] B. W. An, E.-J. Gwak, K. Kim, Y.-C. Kim, J. Jang, J.-Y. Kim, J.-U. Park, *Nano Lett.* **2016**, *16*, 471.
[9] H. Jiang, H. Wang, G. Liu, Z. Su, J. Wu, J. Liu, X. Zhang, Y. Chen, W. Zhou, *J. Alloys Compd.* **2017**, *699*, 1049.
[10] Y. Cheng, H. Zhang, R. Wang, X. Wang, H. Zhai, T. Wang, Q. Jin, J. Sun, *ACS Appl. Mater. Interfaces* **2016**, *8*, 32925.
[11] R. Zhou, P. Li, Z. Fan, D. Du, J. Ouyang, *J. Mater. Chem. C* **2017**, *5*, 1544.
[12] M. C. Zhang, C. Y. Wang, X. P. Liang, Z. Yin, K. L. Xia, H. M. Wang, M. Q. Jian, Y. Y. Zhang, *Adv. Electron. Mater.* **2017**, *3*, 1700193.
[13] S. F. Nadler, K. Weingand, R. J. Kruse, *Pain Physician* **2004**, *7*, 395.
[14] J. M. Mayer, V. Mooney, L. N. Matheson, G. N. Erasala, J. L. Verna, B. E. Udermann, S. Leggett, *Arch. Phys. Med. Rehabil.* **2006**, *87*, 1310.
[15] N. Lazarus, B. Hanrahan, *Adv. Mater. Technol.* **2016**, *1*, 1600130.
[16] M. Amjadi, K.-U. Kyung, I. Park, M. Sitti, *Adv. Funct. Mater.* **2016**, *26*, 1678.
[17] S. Yao, Y. Zhu, *Nanoscale* **2014**, *6*, 2345.
[18] J. A. Fan, W.-H. Yeo, Y. Su, Y. Hattori, W. Lee, S.-Y. Jung, Y. Zhang, Z. Liu, H. Cheng, L. Falgout, M. Bajema, T. Coleman, D. Gregorie, R. J. Larsen, Y. Huang, J. A. Rogers, *Nat. Commun.* **2014**, *5*, 3266.
[19] R. Wang, Z. Xu, J. Zhuang, Z. liu, L. Peng, Z. Li, Y. Liu, W. Gao, C. Gao, *Adv. Electron. Mater.* **2017**, *3*, 1600425.
[20] H. Zhai, R. Wang, X. Wang, Y. Cheng, L. Shi, J. Sun, *Nano Res.* **2016**, *9*, 3924.
[21] J. Jang, B. G. Hyun, S. Ji, E. Cho, B. W. An, W. H. Cheong, J.-U. Park, *NPG Asia Mater.* **2017**, *9*, e432.
[22] B. Yoo, Y. Kim, C. J. Han, M. S. Oh, J.-W. Kim, *Appl. Surf. Sci.* **2018**, *429*, 151.
[23] J.-G. Lee, J.-H. Lee, S. An, D.-Y. Kim, T.-G. Kim, S. S. Al-Deyab, A. L. Yarin, S. S. Yoon, *J. Mater. Chem. A* **2017**, *5*, 6677.
[24] J. Kang, H. Kim, K. S. Kim, S.-K. Lee, S. Bae, J.-H. Ahn, Y.-J. Kim, J.-B. Choi, B. H. Hong, *Nano Lett.* **2011**, *11*, 5154.
[25] H.-S. Jang, S. K. Jeon, S. H. Nahm, *Carbon* **2011**, *49*, 111.
[26] D. Jung, D. Kim, K. H. Lee, L. J. Overzet, G. S. Lee, *Sens. Actuators, A* **2013**, *199*, 176.
[27] J. Luo, H. Lu, Q. Zhang, Y. Yao, M. Chen, Q. Li, *Carbon* **2016**, *110*, 343.
[28] J. Zhou, M. Mulle, Y. Zhang, X. Xu, E. Li, F. Han, S. T. Thoroddsen, G. Lubineau, *J. Mater. Chem. C* **2016**, *4*, 1238.
[29] Z. Yu, J. Shang, X. H. Niu, Y. W. Liu, G. Liu, P. Dhanapal, Y. N. Zheng, H. L. Yang, Y. Z. Wu, Y. L. Zhou, Y. X. Wang, D. X. Tang, R.-W. Li, *Adv. Electron. Mater.* **2018**, *4*,1800137.
[30] M. D. Dickey, *Adv. Mater.* **2017**, *29*, 1606425.
[31] N. Kazem, T. Hellebrekers, C. Majidi, *Adv. Mater.* **2017**, *29*, 1605985.
[32] Y. X. Wang, Z. Yu, J. Shang, Y. W. Liu, R.-W. Li, *Res. Dev. Mater. Sci.* **2018**, *5*, 000617.
[33] J. Park, S. D. Wang, M. Li, C. Ahn, J. K. Hyun, D. S. Kim, D. K. Kim, J. A. Rogers, Y. G. Huang, S. Jeon, *Nat. Commun.* **2012**, *3*, 916.
[34] S. Liang, Y. Li, Y. Chen, J. Yang, T. Zhu, D. Zhu, C. He, Y. Liu, S. Handschuh-Wang, X. Zhou, *J. Mater. Chem. C* **2017**, *5*, 1586.
[35] S. Yao, Y. Zhu, *Adv. Mater.* **2015**, *27*, 1480.
[36] D. McCoul, W. Hu, M. Gao, V. Mehta, Q. Pei, *Adv. Electron. Mater.* **2016**, *2*, 1500407.
[37] S. Choi, S. I. Han, D. Jung, H. J. Hwang, C. Lim, S. Bae, O. K. Park, C. M. Tschabrunn, M. Lee, S. Y. Bae, J. W. Yu, J. H. Ryu, S.-W. Lee, K. Park, P. M. Kang, W. B. Lee, R. Nezafat, T. Hyeon, D.-H. Kim, *Nat. Nanotechnol.* **2018**, https://doi.org/10.1038/s41565-018-0226-8.
[38] J. Jiang, B. Bao, M. Li, J. Sun, C. Zhang, Y. Li, F. Li, X. Yao, Y. Song, *Adv. Mater.* **2016**, *28*, 1420.
[39] M. Su, Z. Huang, Y. Li, X. Qian, Z. Li, X. Hu, Q. Pan, F. Li, L. Li, Y. Song, *Adv. Mater.* **2018**, *30*, 1703963.
[40] Z. Cui, Y. Han, Q. Huang, J. Dong, Y. Zhu, *Nanoscale* **2018**, *10*, 6806.
[41] C. Liu, N. Huang, F. Xu, J. Tong, Z. Chen, X. Gui, Y. Fu, C. Lao, *Polymers* **2018**, *10*, 629.
[42] D. Wang, Y. Zhang, X. Lu, Z. Ma, C. Xie, Z. Zhang, *Chem. Soc. Rev.* **2018**, *47*, 4611.
[43] H. Yuk, X. Zhao, *Adv. Mater.* **2018**, *30*, 1704028.
[44] A. D. Valentine, T. A. Busbee, J. W. Boley, J. R. Raney, A. Chortos, A. Kotikian, J. D. Berrigan, M. F. Durstock, J. A. Lewis, *Adv. Mater.* **2017**, *29*, 1703817.
[45] G. Li, D.-W. Lee, *Lab Chip* **2017**, *17*, 3415.
[46] T. Lu, J. Wissman, Ruthika, C. Majidi, *ACS Appl. Mater. Interfaces* **2015**, *7*, 26923.